



Universiteit  
Leiden  
The Netherlands

## **Lipid bilayers decorated with photosensitive ruthenium complexes**

Bahreman, A.

### **Citation**

Bahreman, A. (2013, December 17). *Lipid bilayers decorated with photosensitive ruthenium complexes*. Retrieved from <https://hdl.handle.net/1887/22877>

Version: Not Applicable (or Unknown)

License: [Leiden University Non-exclusive license](#)

Downloaded from: <https://hdl.handle.net/1887/22877>

**Note:** To cite this publication please use the final published version (if applicable).

Cover Page



Universiteit Leiden



The handle <http://hdl.handle.net/1887/22877> holds various files of this Leiden University dissertation

**Author:** Bahreman, Azadeh

**Title:** Lipid bilayers decorated with photosensitive ruthenium complexes

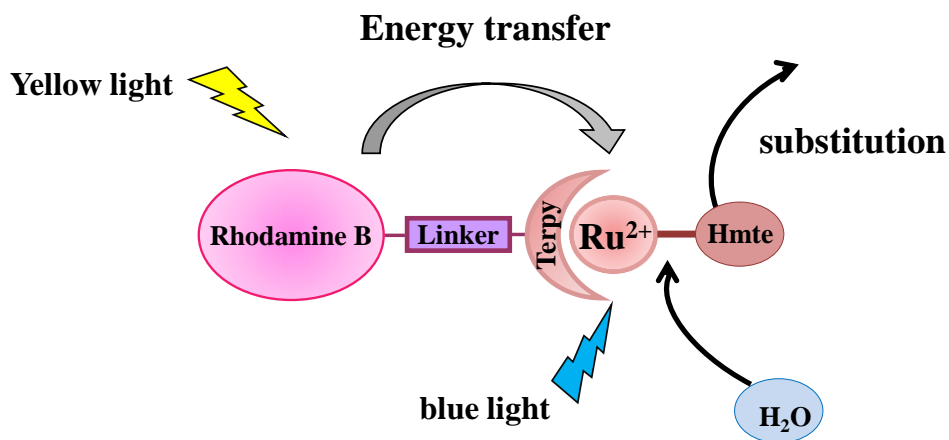
**Issue Date:** 2013-12-17

# 6

---

---

## Yellow-light sensitization of a ligand photosubstitution reaction in a ruthenium polypyridyl complex covalently bound to a rhodamine dye



**Abstract**

The ruthenium complex  $[\text{Ru}(\text{terpy})(\text{bpy})(\text{Hmte})]^{2+}$  ( $[\mathbf{1}]^{2+}$ ), where terpy is 2,2',6',2''-terpyridine, bpy is 2,2'-bipyridine, and Hmte is 2-methylthioethan-1-ol, poorly absorbs yellow light, and although its quantum yield for the photosubstitution of Hmte by water is comparable at 570 nm and at 452 nm (0.011(4) vs. 0.016(4) at 298 K at neutral pH), the photoreaction using yellow photons is very slow. Complex  $[\mathbf{1}]^{2+}$  was thus functionalized with rhodamine B, an organic dye known for its high extinction coefficient for yellow light. Complex  $[\text{Ru}(\text{Rterpy})(\text{bpy})(\text{Hmte})]^{3+}$  ( $[\mathbf{2}]^{3+}$ ) was synthesized, where Rterpy is a terpyridine ligand covalently bound to rhodamine B *via* a short saturated linker.  $[\mathbf{2}]\text{Cl}_3$  shows a very high extinction coefficient at 570 nm ( $44000 \text{ M}^{-1}\cdot\text{cm}^{-1}$ ), but its luminescence upon irradiation at 570 nm is completely quenched in aqueous solution. The quantum yield for the photosubstitution of Hmte by water in  $[\mathbf{2}]^{3+}$  was comparable to that in  $[\mathbf{1}]^{2+}$  at 570 nm (0.0085(6) vs. 0.011(4), respectively), which, in combination with the much higher extinction coefficient, resulted in a higher photosubstitution rate constant for  $[\mathbf{2}]^{3+}$  than for  $[\mathbf{1}]^{2+}$ . The energy of yellow photons is thus transferred efficiently from the rhodamine antenna to the ruthenium center, leading to efficient photosubstitution of Hmte. These results bring new opportunities for extending the photoactivation of polypyridyl ruthenium complexes towards longer wavelengths.

## 6.1. Introduction

Ruthenium polypyridyl complexes are known for their rich photochemistry, which often requires blue light irradiation.<sup>[1-7]</sup> In such complexes, photon absorption into a Metal-to-Ligand Charge-Transfer band (<sup>1</sup>MLCT) typically situated between 400 and 500 nm, leads to the corresponding <sup>3</sup>MLCT state *via* intersystem crossing. If the distortion of the octahedral coordination geometry is sufficient to decrease the ligand field splitting energy, further thermal population of the Metal-Centered excited states (<sup>3</sup>MC) may result in ligand photosubstitution reactions.<sup>[8-11]</sup> Recently, this type of photoactive metal complexes have been proposed as light-activated drugs in phototherapy, as the aqua photoproducts may typically interact with biomolecules and lead to significant cytotoxicity, whereas the initial complex may not.<sup>[12-21]</sup> As has been shown in the literature dealing with Photodynamic Therapy (PDT)<sup>[22-24]</sup> light activation allows for controlling the amount of reactive oxygen species produced locally, which may contribute to limiting toxicity and side-effects during chemotherapy. On the other hand, blue light irradiation *in vivo* has a rather limited applicability for PDT since its tissue penetration is low.<sup>[25-26]</sup> The fact that the MLCT band of most polypyridyl ruthenium complexes is located in the blue region has been restricting, up to now, real phototherapeutic applications of these complexes. Thus, it is of great interest to make the photoactivation of ruthenium polypyridyl complexes possible with photons of longer wavelengths, without sacrificing the complex stability in the dark, which is an important requirement in photochemotherapy.

One strategy, recently reviewed by Brewer *et al.*,<sup>[27]</sup> is to design complexes having their MLCT band at higher wavelengths. Such strategy sometimes lowers the stability of the complexes in the dark, but a few complexes have been published that are reasonably stable in the dark and photoactive using red light. A second strategy is the coordination of a fluorescent ligand to the ruthenium center in order to sensitize the metal complex with photons of higher wavelength. Mascharak and co-workers<sup>[28-30]</sup> have used this strategy to bring the sensitization of ruthenium nitrosyl compounds from the UV to the visible region. Typically, direct coordination of the fluorophore to ruthenium promotes merging of the absorption band of both fragments, thus shifting light activation of the metal center towards higher wavelengths.<sup>[31]</sup> A third, somewhat similar strategy, is to link the fluorophore to the ruthenium complex *via* a non-conjugated linker and to use the “reverse” FRET effect.

Efficient Förster energy transfer (FRET) from a fluorophore to a ruthenium center is typically obtained when the <sup>1</sup>MLCT absorption band of the ruthenium complex overlaps well with the emission band of the fluorophore. The efficiency of FRET is also related to the distance between the energy donor and the energy acceptor.<sup>[32-34]</sup> When the maximum of the emission spectrum of the dye is at lower wavelength than the absorption maximum of the ruthenium complex, forward FRET is obtained.<sup>[35-37]</sup> However, for phototherapeutic application, photoactivation of the ruthenium complex *via* forward FRET, *i.e.*, with photons of low wavelength, is not suitable, and “reverse FRET” from a fluorophore with an emission maximum at a higher wavelength than that of the absorption maximum of the ruthenium moiety, is preferable.<sup>[34]</sup> Etchenique and co-workers recently introduced this strategy by coordinating a green-emitting, rhodamine B-functionalized nitrile ligand to a chlorido- bis(bipyridine)ruthenium(II) compound. The use of a saturated linker avoided orbital overlap between the dye and the complex, and green light irradiation was shown to result in photosubstitution of the nitrile ligand, thus releasing the fluorophore from the ruthenium complex.<sup>[38]</sup>

We report here a new photoactivatable system relying on reverse FRET, in which coupling of the rhodamine B dye is realized at the 4' position of a spectator terpyridine ligand that is not released upon light irradiation (Figure 6.1). The photosubstitution of the thioether Hmte ligand by an aqua ligand in complex [Ru(terpy)(bpy)(Hmte)]<sup>2+</sup> (compound [1]<sup>2+</sup>, where terpy is 2,2',6',2''-terpyridine, bpy is 2,2'-bipyridine, and Hmte is 2-methylthioethan-1-ol) is reported in Chapter 3. The absorption spectrum of [1]<sup>2+</sup> extends up to 610 nm and only slightly overlaps with the emission band of rhodamine B ( $\lambda_{em}$ =570 nm) (Figure 6.1b). The rhodamine B-functionalized analogue complex [2]<sup>3+</sup> (Figure 6.1c) may thus allow energy transfer from the fluorophore to the ruthenium center to occur, thus leading to efficient ligand photosubstitution. The high extinction coefficient of the organic dye may allow for more efficient photon collection and thus faster photosubstitution of Hmte when excited near 600 nm, compared to complex [1]<sup>2+</sup>. In this Chapter, the rate and quantum yield for the photosubstitution of Hmte in the analogous ruthenium complexes [1]<sup>2+</sup> and [2]<sup>3+</sup> are compared upon both yellow (570 nm) and blue (450 nm) light irradiation, in order to investigate the efficiency of photosensitization on the Ru-based ligand exchange process.

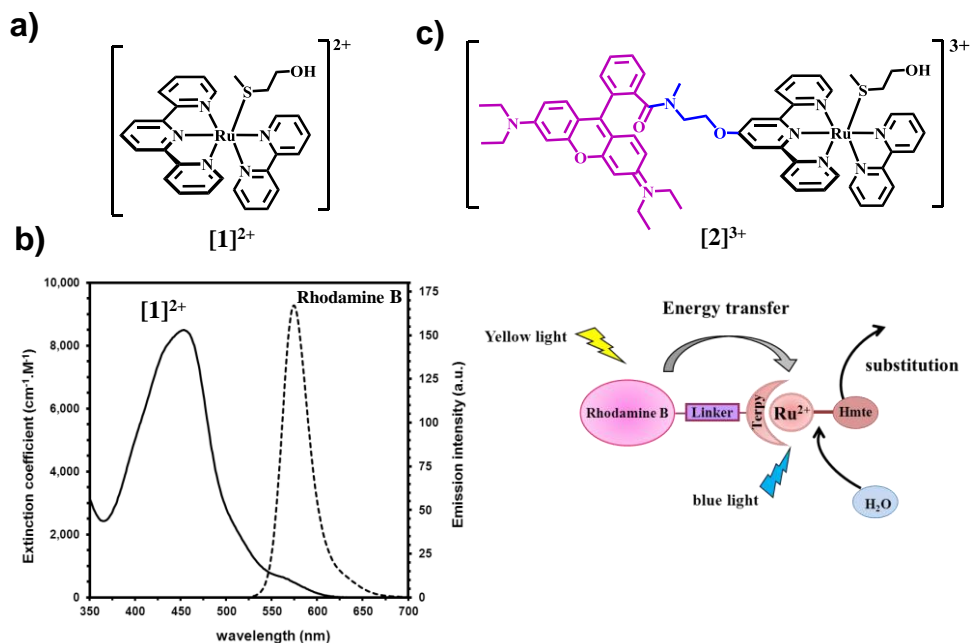


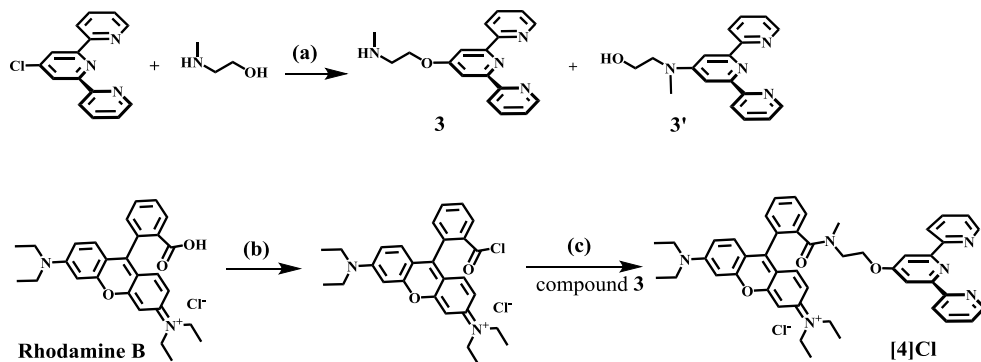
**Figure 6.1.** a) Chemical structure of  $[Ru(terpy)(bpy)(Hmte)]^{2+}$  ( $[1]^{2+}$ ). b) Absorption spectrum of  $[1]^{2+}$  (left axis) and emission spectrum of rhodamine B (right axis). c) Chemical structure of the rhodamine B-functionalized ruthenium complex  $[2]^{3+}$  and photochemical scheme.

## 6.2. Results

### 6.2.1. Synthesis

In order to couple a rhodamine B molecule to the 4' position of the 2,2',6',2''-terpyridine (terpy) ligand an ethanolamine linker may seem at first sight appropriate. However, in basic conditions the secondary amide bond resulting from coupling between the primary amine of ethanolamine and the carboxylic acid of rhodamine B, cyclizes to a spirolactame, which leads to quenching of the fluorescence of the dye.<sup>[39-40]</sup> Thus, a secondary amine, 2-methylaminoethanol, was used instead, because the resulting tertiary amide cannot be deprotonated and cyclize into the spiro compound. The synthetic route towards ligand **[4]Cl** is shown in Scheme 6.1. In the first step, a literature procedure was modified<sup>[41]</sup> to substitute the chloride substituent of 4'-chloro-2,2',6',2''-terpyridine by 2-methylaminoethanol using KOH as a base, to form compound **3**. Two structural isomers, compounds **3** (O-bound) and **3'** (N-bound) (Scheme 6.1) can be formed depending on the amount of base, on the temperature, and

on the reaction time. By using a relatively low amount of KOH (2.8 eq) and short reaction times no side product **3'** was detected by  $^1\text{H}$  NMR of the crude product, and compound **3** could be further functionalized.

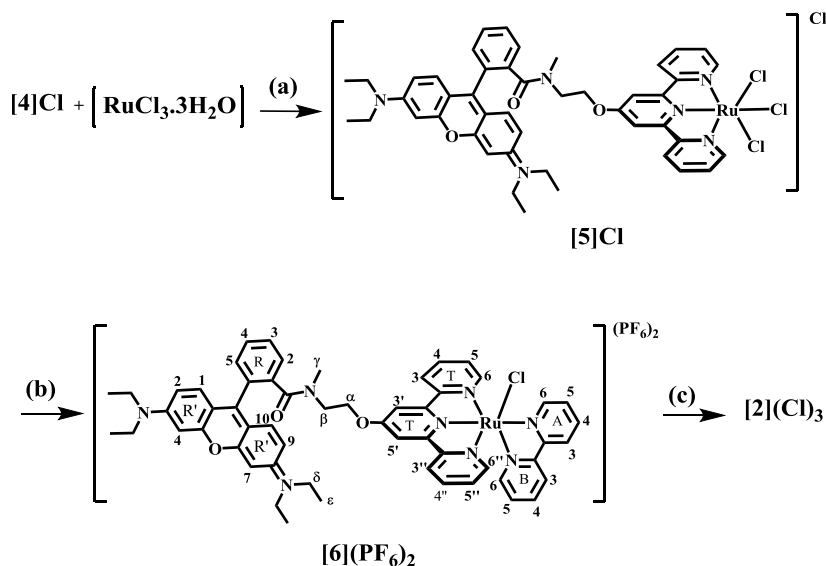


**Scheme 6.1.** Synthetic procedure towards compound **3** and **[4]Cl**. (a) KOH, DMSO (dry), heating at 60 °C for 3 h, overnight at R.T. Yield of **3**: 87% (b) POCl<sub>3</sub>, C<sub>2</sub>H<sub>4</sub>Cl<sub>2</sub> (dry), reflux, 5 h. (c) I: Et<sub>3</sub>N, CH<sub>3</sub>CN (dry), reflux, 14h, II: KPF<sub>6</sub> in water, III: chloride exchange DOWEX resin, acetone:H<sub>2</sub>O (1:1), 4 h, r.t. Yield: 31% (from compound **3**).

In the second step, rhodamine B was coupled to **3** following a modified literature procedure<sup>[42]</sup> involving the acid chloride of rhodamine B and **3** using Et<sub>3</sub>N as a base in acetonitrile. After precipitation from water using PF<sub>6</sub><sup>-</sup> as a counter ion, full water solubility was recovered by anion exchange to Cl<sup>-</sup> using an anion exchange resin. Column chromatography on silica gel allowed removing the unreacted rhodamine B to afford compound **[4]Cl** as a purple solid with an overall yield of 31%. The UV-vis spectrum of **[4]Cl** in water (Figure 6.2a and Table 6.1) showed a red shift of the  $\pi$ - $\pi^*$  absorption band of about 14 nm ( $\lambda_{abs}$ =569 nm), compared to rhodamine B.

Adapting known synthetic procedures<sup>[43-45]</sup> the ruthenium complex **[2]Cl<sub>3</sub>** was synthesized as shown in Scheme 6.2. Refluxing a mixture of ligand **[4]Cl** with RuCl<sub>3</sub>·3H<sub>2</sub>O in methanol resulted in the paramagnetic complex **[5]Cl**. Product formation was followed by TLC and the final product was characterized by paramagnetic  $^1\text{H}$  NMR and ESI-MS spectrometry. The unpaired electron of the Ru(III) complex generates short relaxation times, which shields the  $^1\text{H}$ - $^1\text{H}$  coupling and thus results in broad NMR signals. This effect is significant for hydrogen atoms of the terpyridine moiety in **[5]Cl** that are close to the paramagnetic ruthenium(III) center. Highly upfield-shifted signals were observed in methanol-d<sub>4</sub> at -1.43 ppm, -10.26

ppm,  $-10.71$  ppm and  $-35.94$  ppm for T33'', T44'', T55'', or T66''. T3' and T5' are more remote from the paramagnetic center and their signals appear at 10.90 ppm.<sup>[46]</sup> The peaks in the 6.90-8.10 ppm region most likely correspond to the rhodamine B moiety and traces of the free ligand [4]Cl. In the ESI-MS spectrum a peak at  $m/z=937.7$  for [5]<sup>+</sup> was found that confirmed the formation of compound [5]Cl.



**Scheme 6.2.** Synthetic route towards ruthenium complexes [5]Cl, [6](PF<sub>6</sub>)<sub>2</sub>, and [2]Cl<sub>3</sub>. (a) MeOH, reflux, 7 h, yield: 54%. (b) I: bpy, LiCl, NEt<sub>3</sub>, EtOH/H<sub>2</sub>O(3:1), reflux, 6 h. II: KPF<sub>6</sub> in water. Yield: 40%. (c) I: Hmte, AgPF<sub>6</sub> (2.6 eq), acetone:H<sub>2</sub>O (5:3), reflux, 9 h. II: chloride exchange DOWEX resin, acetone:H<sub>2</sub>O (1:1), 4 h, r.t. Yield: 43%.

In a second step, the complex [Ru(4)(bpy)(Cl)](PF<sub>6</sub>)<sub>2</sub> ([6](PF<sub>6</sub>)<sub>2</sub>) was obtained as a purple solid via treatment of [5]Cl with 2,2'-bipyridine in presence of EtN<sub>3</sub> and LiCl in an ethanol/water mixture, followed by column chromatography and precipitation with aqueous KPF<sub>6</sub>. Finally, the water soluble, potentially photosensitive ruthenium complex [Ru(4)(bpy)(Hmte)]Cl<sub>3</sub> ([2]Cl<sub>3</sub>) was synthesized by removal of the chloride ligand in [6](PF<sub>6</sub>)<sub>2</sub> using AgPF<sub>6</sub> in presence of an excess of Hmte at elevated temperatures. The PF<sub>6</sub><sup>-</sup> counter ions were then exchanged using a chloride-loaded exchange resin, to form the purple, water-soluble complex [2]Cl<sub>3</sub>. <sup>1</sup>H NMR in methanol-d<sub>4</sub> showed that the protons of the coordinated Hmte ligand (3.46, 1.81, and 1.36 ppm) are shielded in [2]Cl<sub>3</sub> compared to free Hmte (3.75, 2.80, and 2.30 ppm).

Moreover, the characteristic aromatic proton for  $[2]Cl_3$  at 9.80 ppm (6A) appears at different chemical shift compared to that in  $[6](PF_6)_2$  (10.28 ppm). The high resolution mass spectrum showed two peaks for the product at  $m/z=360.45780$  ( $[2]^{3+}$ ) and at  $m/z=540.18289$  ( $[2-H]^{2+}$ ). Overall the analogous complexes  $[2]Cl_3$  and  $[1](BF_4)_2$ , which was synthesized as reported in Chapter 3, are soluble enough in water for studying their photophysical properties and the photosensitivity of their Ru-S bond.

### 6.2.2. Emission measurements

The As reported by Etchenique et al. for a similar rhodamine-ruthenium system,<sup>[38]</sup> even though the overlap between the emission spectrum of the rhodamine B dye and the absorption spectrum of the ruthenium complex  $[1]^{2+}$  is rather small (see Figure 6.1b) the use of a very short linker in  $[2]^{3+}$  was expected to allow at least some of the energy absorbed by rhodamine B to be donated to the ruthenium center in the covalent dyad. The emission and absorption spectra of  $[2]Cl_3$  were measured in water and compared to that of  $[4]Cl$  and rhodamine B (Figure 6.2b). All compounds absorb strongly in the yellow region, with extinction coefficient diminished in  $[4]Cl$  and  $[2]Cl_3$ , however, compared to rhodamine (Table 6.1). In addition, the emission spectrum of  $[2]Cl_3$  shows almost complete quenching of the fluorescence of the rhodamine B group upon excitation of  $[2]Cl_3$  at 570 nm. This effect is not observed in the spectrum of ligand  $[4]Cl$ , which keeps a significant part of the rhodamine fluorescence (Figure 6.2b and Table 6.1). Thus, the energy absorbed by the rhodamine B substituent at 570 nm is either transferred to the ruthenium center by energy transfer, or wasted via non-radiative decay. If energy transfer to the ruthenium complex is efficient, it may lead to the photosubstitution of Hmte by an aqua ligand. ( $\lambda_{max} \sim 450$  nm).

**Table 6.1.** Spectroscopic data in MilliQ water for compounds  $[2]Cl_3$ ,  $[4]Cl$ , and rhodamine B. Emission data were obtained upon excitation at  $\lambda=570$  nm.

Compound	$\epsilon(\lambda_{Max})$ ( $M^{-1} \cdot cm^{-1}$ )	$\lambda_{max}$ (abs) (nm)	$\lambda_{max}$ (em) (nm)
rhodamine B	120000	555	576
$[4]Cl$	74000	569	586
$[2]Cl_3$	44000	570	585

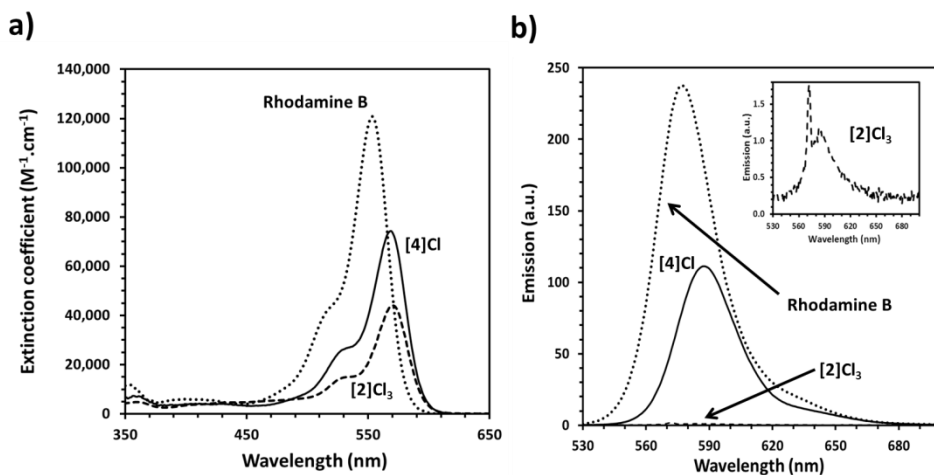
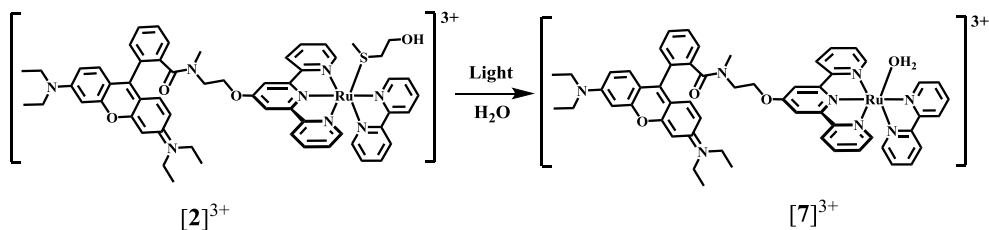


**Figure 6.2.** Absorption (a) and emission (b) spectra of rhodamine B, rhodamine B-terpyridine conjugate [4]Cl, and rhodamine B-functionalized ruthenium complex [2]Cl<sub>3</sub> in MilliQ water at pH=7. Excitation: 570 nm, slit width: 3 nm. The concentrations of the solutions used for emission measurements were chosen so that their absorbance at 570 nm were identical in the three solutions ( $A_{570}=0.23$ ).

### 6.2.3. Photochemistry

The photoreactivity of [2]<sup>3+</sup> (hereafter RuHmte) was investigated by looking at whether the Hmte ligand could be photosubstituted by an aqua ligand, upon either yellow or blue light irradiation in water. The formation of the aqua complex [7]<sup>3+</sup> (see Scheme 6.3) was first monitored by <sup>1</sup>H NMR spectroscopy in D<sub>2</sub>O. NMR samples containing [2]Cl<sub>3</sub> in degassed D<sub>2</sub>O were prepared, and the samples were irradiated with blue ( $\lambda_e = 452$  nm) or yellow light ( $\lambda_e = 570$  nm) at room temperature. While the <sup>1</sup>H NMR spectrum of a reference sample in the dark did not change, the spectra of the irradiated samples showed the gradual disappearance of the starting compound [2]<sup>3+</sup> ( $\delta=9.76$  ppm for proton 6A (see Scheme 6.2), and  $\delta=3.48$  ppm, 1.83 ppm, and 1.37 ppm for coordinated Hmte) and the formation of a single new ruthenium complex ( $\delta=9.61$  ppm for proton 6A) and of the free Hmte ligand (at  $\delta=3.74$ , 2.66, and 2.01 ppm). Figure 6.3 shows the evolution of the <sup>1</sup>H NMR spectra for proton 6A upon irradiation (the complete spectra before and after irradiation are shown in Figure AVI.1). Mass spectra after irradiation were obtained for both samples, and the peak found at 339.6 is characteristic for the formation of [Ru(4)(bpy)(D<sub>2</sub>O)]<sup>3+</sup>. Integration of the protons 6A for [2]<sup>3+</sup> and [7]<sup>3+</sup> indicated typically 40% photoconversion of [2]<sup>3+</sup> to [7]<sup>3+</sup> after about

500 min irradiation. The present data show that a substantial amount of Hmte is indeed photosubstituted, not only upon blue light irradiation but also upon yellow light irradiation, which is absorbed by the rhodamine dye more than by the ruthenium fragment (see below). However, these NMR experiments could not provide quantitative information on the quantum efficiency of the light-induced substitution reaction, as light intensities in the irradiation setup were difficult to determine.



**Scheme 6.3.** Photosubstitution of Hmte in  $[2]^{3+}$  by an aqua ligand upon blue light ( $\lambda=452$  nm) or yellow light ( $\lambda=570$  nm) irradiation in aqueous solution.

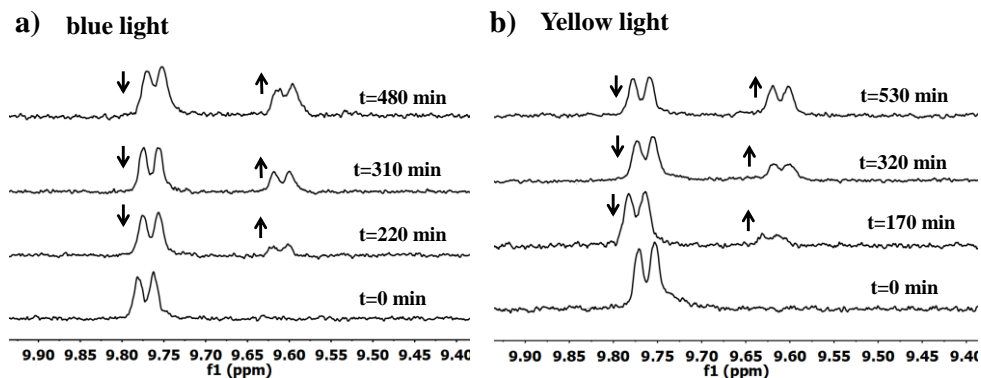


**Figure 6.3.** Evolution of the  $^1\text{H}$  NMR spectra of degassed  $\text{D}_2\text{O}$  solution of  $[2]\text{Cl}_3$  upon irradiation with a) blue light ( $\lambda_e=452$  nm,  $\Delta\lambda_{1/2}=8.9$  nm) or b) yellow light ( $\lambda_e=570$  nm,  $\Delta\lambda_{1/2}=8.9$  nm). Irradiation times are indicated for each spectrum. Conditions: total ruthenium concentration  $[\text{Ru}]_{\text{tot}}=5.3\times 10^{-3}$  M, room temperature.

In order to get quantitative information about the yellow and blue light-triggered release of Hmte from complex  $[2]^{3+}$ , UV-vis experiments were performed in well-controlled irradiation conditions. An aqueous solution of  $[2]\text{Cl}_3$  was exposed to yellow light (570 nm) or blue light (452 nm) *via* a fiber optic bundle bringing light to the top of a UV-vis cuvette, *i.e.* inside the spectrophotometer and perpendicularly to its optical

axis (see Appendix I, Figure AI.1). The UV-vis spectra were measured during light irradiation (Figure 6.4a). The absorption spectrum of the solution gradually evolved until a steady state was obtained after 150 and 320 minutes of irradiation with yellow and blue light, respectively. Isosbestic points at 380 nm, 460 nm, and 557 nm indicate the occurrence of only one photochemical reaction. From the  $^1\text{H}$  NMR and mass spectrometry studies it is clear that extensive irradiation of  $[\mathbf{2}]^{3+}$  leads to the full photoconversion into the aqua complex  $[\mathbf{7}]^{3+}$  ( $\text{RuOH}_2$ ) (see Appendix VI, Figure AVI.2). Thus, in each experiment the concentration of  $[\mathbf{2}]^{3+}$  and  $[\mathbf{7}]^{3+}$  could be calculated from the extinction coefficients of both species (see Appendix I, section AI.2.1). Using Equation 6.1, the photochemical substitution first-order rate constants  $k_{\varphi 570}$  and  $k_{\varphi 452}$  could be obtained from the slope of a plot of  $\ln([\text{RuHmte}]/[\text{Ru}]_{\text{tot}})$  vs. irradiation time (Figure 6.5a-I and II), where  $[\text{RuHmte}]$  and  $[\text{Ru}]_{\text{tot}}$  represent the concentration in  $[\mathbf{2}]^{3+}$  and the total ruthenium concentration in the solution, respectively. Half-reaction times were calculated using Equation 6.2. The data are reported in Table 6.2; they show that the photoconversion rate upon yellow light irradiation,  $k_{\varphi 570}$ , was twice higher compared to that obtained upon blue light irradiation ( $k_{\varphi 452}$ ). Since the photon flux values at 570 nm and 452 nm ( $\Phi_{570}$  and  $\Phi_{452}$ ) were not equal, the rate constants  $k_{\varphi 570}$  and  $k_{\varphi 452}$  cannot be directly compared, but the photosubstitution quantum yields have to be calculated instead. As expressed in Equation 6.3, the photosubstitution rate constant depends on the photon flux  $\Phi$ , the extinction coefficient of RuHmte at the irradiation wavelength  $\varepsilon^{\lambda_e}$ , the absorbance along the irradiation axis at the irradiation wavelength  $3A_e$  (see Appendix I, Figure AI.1), the probability of absorbance of the photon ( $1 - 10^{-3A_e}$ ), the photosubstitution quantum yield  $\varphi$ , the absorption pathlength  $l$ , and the irradiated volume  $V$ .

$$-\frac{dn_{\text{RuHmte}}}{dt} = \frac{dn_{\text{RuOH}_2}}{dt} = k_{\varphi} \cdot n_{\text{RuHmte}} \quad \text{(Equation 6.1)}$$

$$t_{1/2} = \frac{\ln 2}{k_{\varphi}} \quad \text{(Equation 6.2)}$$

$$k_{\varphi} = \Phi \cdot (1 - 10^{-3A_e}) \cdot \left( \frac{\varepsilon^{\lambda_e} \cdot l}{A_e \cdot V} \right) \cdot \varphi \quad \text{(Equation 6.3)}$$

The number of moles of RuHmte remaining in solution,  $n_{\text{RuHmte}}$ , was plotted vs. the number of moles of photons  $Q$  absorbed at time  $t$  since  $t=0$  by RuHmte (Figure 6.5b

and Appendix I, section AI.3.2). The photosubstitution quantum yields were obtained directly from the slope of these plots; they were found to be  $8.5(6)\times 10^{-3}$  and  $9.2(7)\times 10^{-3}$  for yellow and blue light irradiation, respectively (Table 6.2). These values are unexpectedly similar, which demonstrates the non-intuitive results that once absorbed, a yellow photon has almost the same probability to lead to ligand photosubstitution as a blue photon.

However, the quantity of  $\text{RuOH}_2$  formed in a given irradiation time depends on the amount of light absorbed by the complex at the irradiation wavelength as well. In this regard, the extinction coefficients of compound  $[\mathbf{2}]^{3+}$  at 570 nm and 452 nm are very different ( $4.4(2)\times 10^4 \text{ M}^{-1}\cdot\text{cm}^{-1}$  and  $4.8(2)\times 10^3 \text{ M}^{-1}\cdot\text{cm}^{-1}$ , respectively). Thus, in order to compare the photosubstitution rates the extinction coefficients must be considered as well. Multiplying the extinction coefficient by the photosubstitution quantum yield gives a value called the photosubstitution reactivity ( $\zeta$ ),<sup>[38]</sup> which best represents how fast a photoreaction will occur under a given photon flux. Actually, Equation 6.3 simplifies into Equation 6.4 when the absorbance  $A_e$  is small compared to 1.

$$k_\varphi \approx \left(\ln 10 \cdot \frac{l}{V}\right) \cdot \Phi \cdot \varepsilon^{\lambda_e} \cdot \varphi = \left(\ln 10 \cdot \frac{l}{V}\right) \cdot \Phi \cdot \xi \quad \text{(Equation 6.4)}$$

The calculated values of  $\zeta$  are reported in Table 6.2. These values show that for complex  $[\mathbf{2}]^{3+}$  Hmte substitution is one order of magnitude faster with yellow light than with blue light. In fact, ten times more moles of photoproduct ( $[\mathbf{7}]^{2+}$ ) were produced upon yellow light irradiation compared to blue light irradiation at short reaction times. Quantitatively, the higher molar absorptivity of the complex  $[\mathbf{2}]^{3+}$  at 570 nm due to the allowed character of the intraligand  $\pi\text{-}\pi^*$  transition of the rhodamine B moiety, promotes intensive absorption of yellow photons compared to blue ones.

In order to evaluate the influence of the rhodamine B antenna on the photosubstitution of Hmte, similar irradiation experiments were performed on complex  $[\mathbf{1}]^{2+}$ , which does not have the fluorophore antenna. Upon yellow light irradiation (570 nm) the absorption band of  $[\mathbf{1}]^{2+}$  at 450 nm gradually disappeared to give rise to a new absorption maximum at higher wavelength corresponding to  $[\text{Ru}(\text{terpy})(\text{bpy})(\text{OH}_2)]^{2+}$  ( $[\mathbf{8}]^{2+}$ , see Figure 6.4b). The first-order photosubstitution rate constant was obtained from the slope of the plots of  $\ln([\text{RuHmte}]/[\text{Ru}]_{\text{tot}})$  vs. irradiation time (Figure 6.5a-III), and the photosubstitution quantum yield was obtained as described above (Figure 6.5b-III). The photosubstitution quantum yield of compound  $[\mathbf{1}]^{2+}$  upon blue light irradiation

was reported in Chapter 3 different irradiation conditions.<sup>[45]</sup> For better comparison with  $[2]^{3+}$  we repeated the measurement in the same irradiation conditions as for  $[2]^{3+}$  (Figure 6.5-IV). All photochemical data, including half-reaction times, are reported in Table 6.2. Like for  $[2]^{3+}$  the photosubstitution quantum yields for  $[1]^{2+}$  upon blue light and yellow light irradiation were found to be very close to each other, *i.e.*, 0.016(4) *vs.* 0.011(4), respectively. This counter-intuitive result confirms our observations on  $[2]^{3+}$ , that once absorbed by  $[1]^{2+}$  yellow photons are able to lead to ligand photosubstitution as efficiently as blue photons.

In order to compare the photoreactivity of different compounds one should compare their  $\zeta$  values, which depends on both the extinction coefficient ( $\epsilon_\lambda$ ) and the photosubstitution quantum yield ( $\phi_\lambda$ ). Although the photosubstitution quantum yields at 570 nm and 452 nm are comparable for both complexes  $[1]^{2+}$  and  $[2]^{3+}$ , the extinction coefficient at 570 nm ( $\epsilon_{570}$ ) is two orders of magnitudes higher for  $[2]^{3+}$  than for  $[1]^{2+}$  due to the presence of the yellow-absorbing dye, while the values of  $\epsilon_{452}$  are of the same order of magnitude for both complexes. As a result, under yellow light irradiation  $\zeta$  is about two orders of magnitude higher for  $[2]^{3+}$  than for  $[1]^{2+}$ , and it is still four times higher than that of  $[1]^{2+}$  under blue light irradiation. Overall, at constant photon flux the different extinction coefficients ( $\epsilon_\lambda$ ) most strongly influence the photosubstitution rate constants for  $[1]^{2+}$  and  $[2]^{3+}$  at 450 or 570 nm, whereas the quantum yields poorly depend on irradiation wavelength.

This result is similar to Kasha's rule, which states that the fluorescence quantum yield of a fluorophore is independent on the irradiation wavelength.<sup>[47]</sup> Indeed, like for fluorophores where emission always occurs from the lowest singlet excited state, for ruthenium complexes such as  $[1]^{2+}$  or  $[2]^{3+}$  photosubstitution is expected to occur from a ruthenium-based  $^3\text{MLCT}$  state *via* thermal promotion to a nearby dissociative  $^3\text{MC}$  state. Reaching the  $^3\text{MLCT}$  state can be done either by direct excitation of the  $^1\text{MLCT}$  band of the ruthenium complex, or by excitation of the rhodamine dye followed by energy transfer to the ruthenium fragment. In the case of a direct excitation of the metal complex ( $[1]^{2+}$ ) yellow photons need to be absorbed by vibrationally excited ground-state complexes, to be able to lead to the  $^3\text{MLCT}$  excited state. Once there, non-radiative decay will occur with almost the same probability as when the  $^3\text{MLCT}$  state is obtained by absorption of blue photons by a non-vibrationally excited ground state complex. In the case of indirect excitation of  $[2]^{3+}$  with yellow photon the  $^3\text{MLCT}$  state is probably reached efficiently *via* absorption by the rhodamine group, followed by

energy transfer. While from Etchenique's work energy transfer was expected to occur in  $[2]^{3+}$ , it was not expected to be *that* efficient.

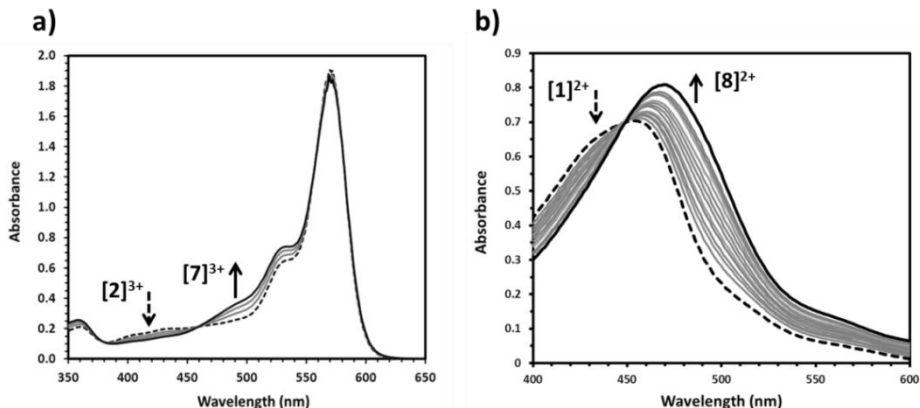


**Figure 6.4.** a) Time evolution of the UV-vis spectrum of an aqueous solution of a)  $[2]^{3+}$  and b)  $[1]^{2+}$  irradiated with yellow light ( $\lambda_e=570$  nm). Condition: photon flux  $\Phi=5.3 \times 10^{-9}$  Einstein $\cdot$ s $^{-1}$ , irradiation pathlength  $l'=3$  cm,  $T=298$  K. Total ruthenium concentrations: a)  $[Ru]_{tot} = 3.4 \times 10^{-5}$  M b)  $[Ru]_{tot} = 1.2 \times 10^{-4}$  M.

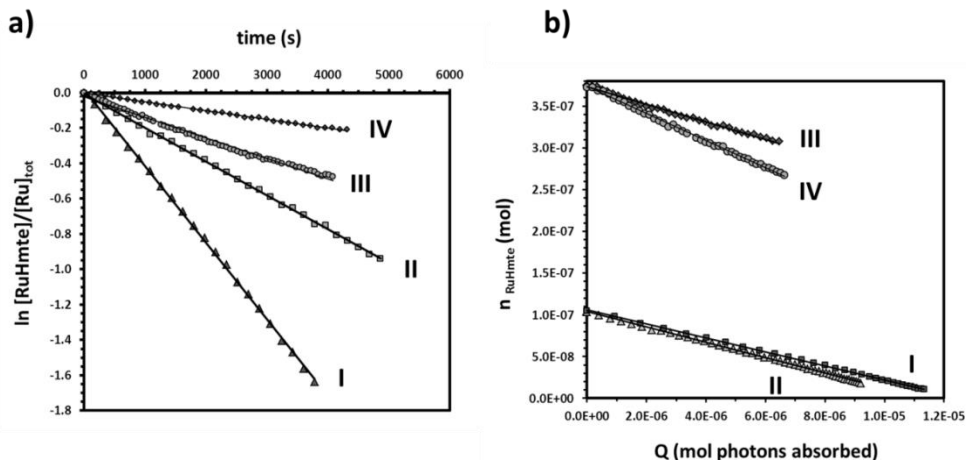


**Figure 6.5.** a) Plots of  $\ln([RuHmte]/[Ru]_{tot})$  vs. irradiation time;  $[RuHmte]$  represents the concentration in  $[2]^{3+}$  or  $[1]^{2+}$ , and  $[Ru]_{tot}$  the total ruthenium concentration in the solution. The slope of each plot is  $k_\phi$  (s $^{-1}$ ). b) Plots of the number of moles of RuHmte vs. the number of moles of photons  $Q$  absorbed by RuHmte at time  $t$ , since  $t=0$ ; the slope is the photosubstitution quantum yield  $\phi$ . I) RuHmte= $[2]^{3+}$ ,  $[Ru]_{tot}=3.4 \times 10^{-5}$  M, yellow light ( $\lambda_e=570$  nm). II) RuHmte= $[2]^{3+}$ ,  $[Ru]_{tot}=3.4 \times 10^{-5}$  M, blue light ( $\lambda_e=452$  nm). III) RuHmte= $[1]^{2+}$ ,  $[Ru]_{tot}=1.2 \times 10^{-4}$  M, yellow light ( $\lambda_e=570$  nm). IV)

RuHmte=[**1**]<sup>2+</sup>,  $[Ru]_{tot}=1.2\times 10^{-4}$  M, blue light ( $\lambda_e=452$  nm). Photon fluxes:  $\Phi_{570}=5.3(8)\times 10^{-9}$  Einstein·s<sup>-1</sup> and  $\Phi_{452}=3.0(6)\times 10^{-9}$  Einstein·s<sup>-1</sup>.

**Table 6.2.** Photochemical data for the photosubstitution of Hmte by H<sub>2</sub>O in [**2**]<sup>3+</sup> and [**1**]<sup>2+</sup> in MilliQ water. Condition:  $T=298$  K, irradiation pathlength  $l=3$  cm, concentration in [**2**]<sup>3+</sup>:  $3.4\times 10^{-5}$  M, concentration in [**1**]<sup>2+</sup>:  $1.2\times 10^{-4}$  M.

Ru complex	$\lambda_e$ (nm)	$\epsilon_{je}$ (M <sup>-1</sup> ·cm <sup>-1</sup> )	$\Phi$ (Einstein·s <sup>-1</sup> )	$k_\phi$ (s <sup>-1</sup> )	$t_{(1/2)}$ (min)	$\phi$	$\xi$ ( $\phi\cdot\epsilon_{je}$ )
[ <b>2</b> ] <sup>3+</sup>	570	44000	$5.3(8)\times 10^{-9}$	$4.4(3)\times 10^{-4}$	26(2)	$8.5(6)\times 10^{-3}$	370(15)
[ <b>2</b> ] <sup>3+</sup>	452	4800	$3.0(6)\times 10^{-9}$	$1.9(3)\times 10^{-4}$	59(2)	$9.2(7)\times 10^{-3}$	44(8)
[ <b>1</b> ] <sup>2+</sup>	570	450	$5.3(8)\times 10^{-9}$	$5.2(2)\times 10^{-5}$	220(5)	$1.1(4)\times 10^{-2}$	4.8(5)
[ <b>1</b> ] <sup>2+</sup>	452	6600	$3.0(6)\times 10^{-9}$	$1.3(4)\times 10^{-4}$	89(3)	$1.6(4)\times 10^{-2}$	100(10)

### 6.3. Discussion

The covalent binding of a rhodamine B dye to the terpy ligand of the ruthenium complex in [**2**]<sup>3+</sup> leads to rather efficient photosensitization, as photosubstitution upon yellow light irradiation became faster even compared to blue light irradiation of the parent complex [**1**]<sup>2+</sup>. Sensitization seems occur via energy transfer from the rhodamine B sensitizer to the <sup>1</sup>MLCT excited state of the ruthenium complex, which is consistent with the work reported by Etchenique.<sup>[38]</sup> By using a short saturated linker, the attachment of rhodamine B to the ruthenium complex occurs without mixing the orbitals of the dye and that of the ruthenium complex. Thus, we assume that the spectrum of [**1**]<sup>2+</sup> is a good model for the contribution of the ruthenium moiety to the spectrum of [**2**]<sup>3+</sup>, *i.e.*, that the excited states of the rhodamine B part and of the ruthenium part in [**2**]<sup>3+</sup> are not too much affected by each other. By comparing the extinction coefficient of [**2**]<sup>3+</sup> with that of [**1**]<sup>2+</sup> in Table 6.2, it appears that only 1% of the yellow photons are absorbed by the ruthenium-centered <sup>1</sup>MLCT band in [**2**]<sup>3+</sup>, while this fraction goes up to 73% for blue photons. In fact, the presence of rhodamine B is not significantly interfering with the MLCT-based blue photon absorption in [**2**]<sup>3+</sup>, whereas, it contributes largely to yellow photon absorption.

Considering on the one hand the emission quenching of the rhodamine B moiety in [**2**]<sup>3+</sup>, and on the other hand the very similar photosubstitution quantum yields upon blue and yellow light irradiation, non-radiative decay in [**2**]<sup>3+</sup> seems to mostly occur

from the  $^3\text{MLCT}$  state of the ruthenium moiety, rather than from the  $S_1$  excited state of the rhodamine B moiety. According to Etchenique's work the energy transfer in  $[\mathbf{2}]^{3+}$  is expected to occur *via* reverse FRET mechanism, *i.e.*, the rather small spectral overlap between the emission of the FRET donor and the absorption of the ruthenium acceptor must be compensated by the very short distance between both components in the dyad. However, other types of energy transfer mechanisms, such as Dexter's,<sup>[32]</sup> cannot be fully ruled out at that stage. Deeper photophysical and theoretical studies would be needed to assess whether direct orbital overlap between the rhodamine antenna and the ruthenium center in  $[\mathbf{2}]^{3+}$  plays a role in the energy transfer process.

From a pure photochemical point of view, such sensitization might find application in photoactivated chemotherapy (PACT), for which the practical efficiency of a given compound will depend on the amount of photoproduct generated in a given irradiation time. Thus, at a given light intensity the photosubstitution quantum yield does not matter too much, but it is the photosubstitution reactivity  $\xi$ , which also takes the extinction coefficient into account, that should be considered. On the other hand, it cannot be forgotten that functionalization of a light-activatable metallodrug with large, flat aromatic dye is expected to change many biological properties of the complex such as its lipophilicity, uptake mechanism, and/or mechanism of cytotoxicity. In the end, only compounds that combine good uptake, a low toxicity in the dark, a high toxicity after ligand substitution, *and* a high photosubstitution reactivity, might be interesting for medicinal purposes.

## 6.4. Conclusions

Our data show that yellow photons that do not seem to have enough energy to populate the  $^1\text{MLCT}$  state of  $[\mathbf{1}]^{2+}$  or  $[\mathbf{2}]^{3+}$  lead, once absorbed, lead to photosubstitution of Hmte with almost the same quantum efficiency as that achieved with blue photons. Thus, for this family of ruthenium compounds Kasha's rule remains valid, *i.e.*, the quantum efficiency of photosubstitution reactions does not depend on the energy of the incoming photons. However, irradiating photosensitive complexes such as  $[\mathbf{1}]^{2+}$  far down their absorption band does render photon collection less efficient. Upon covalent attachment of an organic dye with high molar absorptivity (here rhodamine B for yellow photons) the absorption problem was solved, and for complex  $[\mathbf{2}]^{3+}$  efficient energy transfer from the dye to the ruthenium center was observed. The resulting

photosubstitution reactivity under yellow light irradiation became even higher than that of compound **[1]**<sup>2+</sup> under blue light irradiation.

To conclude, it may be noted that sensitizing the ruthenium complex with dyes absorbing at still higher wavelengths, *i.e.*, up in the red region, might become increasingly difficult. The efficiency of energy transfer is expected to decrease when the spectrum overlap between the emission of the dye and the MLCT band of the ruthenium complex becomes smaller, as a result of which sensitization might not remain possible with dyes that absorb too far in the red region. In the extreme case of negligible spectral overlap, the photoreactivity of the metal center and the emission of the fluorophore are expected to decouple. In such a case, the absorbed photons are expected to lead either to ligand photosubstitution or to fluorescence, depending on the irradiation wavelength. Such systems might find potential application in molecular imaging, for example to probe the position of a ruthenium complex and follow its fate, either in biological or in artificial systems.<sup>[18, 48]</sup>

## 6.5. Experimental section

### 6.5.1. General

<sup>1</sup>H and <sup>13</sup>C NMR spectra were recorded using a Bruker DPX-300 spectrometer; chemical shifts are indicated in ppm relative to TMS. Electrospray mass spectra were recorded on a Finnigan TSQ-quantum instrument by using an electrospray ionization technique (ESI-MS). High resolution mass spectrometry was performed using a Thermo Finnigan LTQ Orbitrap mass spectrometer equipped with an electrospray ion source (ESI) in positive mode (source voltage 3.5 kV, sheath gas flow 10, capillary temperature 275 °C) with resolution R = 60.000 at m/z = 400 (mass range = 150-200) and dioctylphthalate (m/z = 391.28428) as "lock mass". UV-vis spectra were obtained on a Varian Cary 50 UV-vis spectrometer. Emission spectra were obtained using Shimadzu RF-5301 spectrofluorimeter. The irradiation setup was a LOT 1000 W Xenon arc lamp, fitted with a 400FH90-50 Andover standard cutoff filter and a Andover 450FS10-50 ( $\lambda_e=452$  nm,  $\Delta\lambda_{1/2}=8.9$  nm) or a 570FS10-50 ( $\lambda_e=570$  nm,  $\Delta\lambda_{1/2}=8.9$  nm) interference filter. DMSO and dichloroethane were dried over CaSO<sub>4</sub> and distilled before use. CH<sub>3</sub>CN was dried using a solvent dispenser PureSolve 400. 4'-Chloro-2,2';6',2''-terpyridine<sup>[49]</sup> and [Ru(terpy)(bpy)(Hmte)](BF<sub>4</sub>)<sub>2</sub> **[1]**(BF<sub>4</sub>)<sub>2</sub> (Chapter 3) were synthesized following literature procedures. AgPF<sub>6</sub>, LiCl, KPF<sub>6</sub> and the anionic exchange resin DOWEX 22 were purchased from Sigma-Aldrich. Triethylamine was purchased from Acros; KOH and POCl<sub>3</sub> were purchased from Merck;

and rhodamine B was purchased from Lambda Physik. The eluent for column chromatography purification of compound [6](PF<sub>6</sub>)<sub>2</sub> was prepared by mixing MeCN, MeOH, and H<sub>2</sub>O 66:17:17 ratio, followed by addition of solid NaCl until saturation was reached.

### 6.5.2. Synthesis

**Compound 3.** 2-methylaminoethanol (45 mg, 0.60 mmol) was added to a suspension of powdered KOH (94 mg, 1.7 mmol) in dry DMSO (2 mL). The mixture was stirred for 30 min at 333 K. 4'-chloro-2,2':6',2''-terpyridine (160 mg, 0.600 mmol) was added and the mixture was stirred at 333 K for 3 h and then overnight at r.t. Then, the mixture was poured onto water (60 mL). The aqueous phase was extracted with DCM (3×30 mL) and the organic phases were combined and dried over MgSO<sub>4</sub>. DCM was evaporated under reduced pressure and the product was left 24 h under high vacuum at 40 °C to remove trace amounts of DMSO. Compound **3** was obtained as pale yellow oil (160 mg, 0.520 mmol, 87% yield). <sup>1</sup>H NMR (300 MHz, CD<sub>3</sub>OD, 298 K, *see Scheme 6.2 for proton attribution*) δ (ppm) 8.61 (d, J = 4.8 Hz, 2H, T66''), 8.54 (d, J = 8.0 Hz, 2H, T33''), 7.96 – 7.87 (m, 4H, T44'''+ T3' + T5'), 7.41 (ddd, J = 7.5, 4.8, 1.1 Hz, 2H, T44''), 4.29 (t, J = 5.2 Hz, 2H, α), 3.00 (t, J = 5.2 Hz, 2H, β), 2.46 (s, 3H, γ). <sup>13</sup>C NMR (75 MHz, CD<sub>3</sub>OD, 298 K) δ (ppm) 168.39 (T4'), 158.32 (T1), 157.03 (T1'), 150.09 (T66''), 138.68 (T3',T5'), 125.43 (T44''), 122.91 (T33''), 108.35 (T44''), 68.18 (α), 50.84 (β), 35.85 (γ). High resolution ES-MS m/z (calc): 307.15589 (307.15516, [M+H]<sup>+</sup>).

**Compound [4]Cl.** Following a literature procedure<sup>[42]</sup> phosphorus oxychloride (60.0 μL, 0.657 mmol) was added to a solution of rhodamine B (150 mg, 0.313 mmol) in dry 1,2-dichloroethane (5 mL). The mixture was refluxed for 5 h. The solvent was evaporated under reduced pressure and the crude mixture was immediately re-dissolved in dry CH<sub>3</sub>CN (10 mL). Et<sub>3</sub>N (131 μL, 0.939 mmol) and compound **3** (96 mg, 0.31 mmol) were added and the mixture was refluxed for 14 h. The solvent was evaporated under reduced pressure at 30 °C and the crude product was dissolved in water and filtered to remove any solid. The product was precipitated by addition of KPF<sub>6</sub>, filtered, washed with H<sub>2</sub>O, and dried in a desiccator at ambient pressure over silica gel blue for 4 h. Exchange of the PF<sub>6</sub><sup>-</sup> counter anions with Cl<sup>-</sup> was achieved by stirring an acetone/water solution (1:1) of the product with the Cl<sup>-</sup> exchange resin DOWEX 22 (2.0 g) for 4 h. The resin was filtered, acetone was evaporated under reduced pressure at 22 °C, and water was removed using a freeze drier. The product was purified by column chromatography on silica gel (CHCl<sub>3</sub>/MeOH, 10% to 20% of MeOH). Solvents were evaporated under reduced pressure and compound [4]Cl was obtained as a purple solid (75 mg, 0.097 mmol, 31%). <sup>1</sup>H NMR (300 MHz, CD<sub>3</sub>OD,

298 K, *see Scheme 6.2 for proton attribution*)  $\delta$  (ppm) 8.77 – 8.70 (m, 4H, T33'', T66''), 8.06 (td,  $J = 7.7, 1.8$  Hz, 2H, T44''), 7.84 – 7.72 (m, 3H, 5R, 4R, 3R), 7.70 (s, 2H, T3', T5'), 7.54 (ddd,  $J = 7.5, 4.8, 1.2$  Hz, 2H, T44''), 7.47 (dd,  $J = 6.5, 1.0$  Hz, 1H, 5R), 7.34 (d,  $J = 9.6$  Hz, 2H, 10R', 1R'), 7.01 (dd,  $J = 9.6, 2.5$  Hz, 2H, 2R', 9R'), 6.44 (d,  $J = 2.4$  Hz, 2H, 4R', 7R'), 3.84 (t,  $J = 4.3$  Hz, 2H,  $\alpha$ ), 3.74 (t,  $J = 4.3$  Hz, 2H,  $\beta$ ), 3.41 (dd,  $J = 13.4, 6.6$  Hz, 8H,  $\delta$ ), 2.96 (s, 3H,  $\gamma$ ), 1.14 (t,  $J = 7.1$  Hz, 12H,  $\epsilon$ ).  $^{13}\text{C}$  NMR (75 MHz,  $\text{CD}_3\text{OD}$ , 298 K)  $\delta$  (ppm) 171.10 (C=O), 167.99 (3R, 8R), 158.80, 158.25, 157.00, 156.87, 156.30, 150.30 (T66''), 138.82 (T55''), 137.59, 133.31 (2R'+9R'), 131.73+131.65 (3R+2R+4R), 131.17, 130.99 (5R), 128.75 (T5'), 125.78 (T44''), 122.89 (T33''), 115.19 (1R'+10R'), 114.43, 108.06 (T'3), 97.19 (4R'+7R'), 68.13 ( $\alpha+\beta$ ), 46.80 ( $\delta$ ), 40.53 ( $\gamma$ ), 12.78 ( $\epsilon$ ). High resolution ES-MS  $m/z$  (calc): 731.37096 (731.37041  $[\text{M}]^+$ ). UV-vis:  $\lambda_{\text{max}}$  ( $\epsilon$  in  $\text{L}\cdot\text{mol}^{-1}\cdot\text{cm}^{-1}$ ) in pure  $\text{H}_2\text{O}$ : 569 nm (74000). Anal. Calcd for  $\text{C}_{46}\text{H}_{47}\text{ClN}_6\text{O}_3\cdot\text{CHCl}_3\cdot\text{H}_2\text{O}$ : C, 62.39; H, 5.57; N, 9.29. Found: C, 61.77; H, 5.75; N, 9.68.

**Compound [5]Cl.** Compound [4]Cl (120 mg, 0.156 mmol) and  $\text{RuCl}_3\cdot 3\text{H}_2\text{O}$  (41 mg, 0.16 mmol) were dissolved in MeOH (20 mL) and refluxed for 7 h under argon. The mixture was first cooled down to room temperature, and then cooled in an ice bath for 30 min and overnight in the fridge. The precipitate was filtered off and air dried to yield [5]Cl as a dark purple powder (83 mg, 0.075 mmol, 54%).  $^1\text{H}$  NMR (300 MHz,  $\text{CD}_3\text{OD}$ , 298 K, *see Scheme 6.2 for proton attribution*)  $\delta$  (ppm) 10.90 (s, T3', T5'), 8.07 – 7.88 (m, 3H), 7.69 (d,  $J = 6.9$  Hz, 2H), 7.55 (d,  $J = 9.4$  Hz, 2H), 7.01 (d,  $J = 9.7$  Hz, 3H), -1.43 (s, T33''/T44''/T55''), -10.26 (s, T33''/T44''/T55''), -10.71 (s, T33''/T44''/T55''), -35.94 (s, T66''). ES-MS  $m/z$  (calc): 938.2 (937.7  $[\text{M}-\text{Cl}]^+$ ).

**Compound [6](PF<sub>6</sub>)<sub>2</sub>.** [5]Cl (78 mg, 0.080 mmol), 2,2'-bipyridine (13 mg, 0.083 mmol), and LiCl (5.0 mg, 0.12 mmol) were mixed in a 3:1 EtOH/H<sub>2</sub>O mixture (15 mL) and the solution was degassed with argon for 5 min, after which Et<sub>3</sub>N (15  $\mu\text{L}$ , 0.10 mmol) was added. The reaction mixture was refluxed under argon for 6 h, and then it was filtered hot over celite. The filtrate was evaporated under reduced pressure. Column chromatography purification was performed over silica gel (eluent: MeCN / MeOH / H<sub>2</sub>O, 66:17:17 saturated in NaCl,  $R_f=0.5$ ). The solvent was evaporated, then the crude product was dissolved in water (50 mL), and precipitated by adding KPF<sub>6</sub> (~1 g). After filtration, washing with water and drying in a desiccator at ambient pressure over silica gel blue for 5 h compound [6](PF<sub>6</sub>)<sub>2</sub> was obtained in 40% yield as a dark purple powder (41 mg, 0.031 mmol).  $^1\text{H}$  NMR (300 MHz,  $\text{CD}_3\text{OD}$ , 298 K, *see Scheme 6.2 for proton notation*)  $\delta$  (ppm) 10.28 (d,  $J = 5.6$  Hz, 1H, 6A), 8.79 (d,  $J = 8.2$  Hz, 1H, 3A), 8.51 (d,  $J = 8.1$  Hz, 3H, 10R' + 1R' + 3B), 8.32 (t,  $J = 8.1$  Hz, 1H, 4A), 8.07 – 7.91 (m, 5H, 2R' + 9R' + 7R' + 5R + 5A), 7.89 – 7.68 (m, 6H, T3' + T5' + 3R + 4B + T33''), 7.47 (d,  $J = 7.6$  Hz, 1H, 2R), 7.44 – 7.31 (m,

5H, 4R'+ 4R + 5B+ T44''), 7.13 – 7.01 (m, 3H, 6B + T55''), 6.71 (d, J = 2.4 Hz, 2H, T66''), 4.02 (t, J = 4.5 Hz, 2H,  $\alpha$ ), 3.88 (d, J = 4.5 Hz, 2H,  $\beta$ ), 3.45 (m, 8H,  $\delta$ ), 3.05 (s, 3H,  $\gamma$ ), 1.31 (t, J = 12.9 Hz, 12H,  $\epsilon$ ).  $^{13}\text{C}$  NMR (75 MHz,  $\text{CD}_3\text{OD}$ , 298 K)  $\delta$  (ppm)  $^{13}\text{C}$  NMR (75 MHz,  $\text{CD}_3\text{OD}$ , 298 K)  $\delta$  171.25 (C=O), 166.26 (3R,8R), 160.55, 160.48, 159.89, 159.07, 159.03, 158.19, 157.10, 153.86 (6A), 153.78, 152.85 (4R'), 138.42 (4R'+ 5R), 137.72 (4A), 137.64, 136.70 (T33''), 133.46 (T44''), 132.43 (2R), 131.99 (T3'), 131.89 (T5'), 130.98 (4B), 129.85 (3R), 128.74 (4R), 128.57 (5B), 127.96 (5A), 127.43 (6B), 125.09 (10R'+1R), 124.85 (3B), 124.58 (3A), 115.40 (T55''), 114.40, 110.89 (2R'+ 9R'), 97.76 (6T + 6''T), 69.91( $\alpha$ +  $\beta$ ), 48.15 ( $\delta$ ), 46.98 ( $\gamma$ ), 13.04 ( $\epsilon$ ). High resolution ESI-MS m/z (calc): 512.15646 (512.15650 [ $\text{M}-2\text{PF}_6$ ] $^{2+}$ ). UV-vis:  $\lambda_{\text{max}}$  ( $\epsilon$  in  $\text{L}\cdot\text{mol}^{-1}\cdot\text{cm}^{-1}$ ) in 9:1 acetone/ $\text{H}_2\text{O}$ :570 nm (58000).

**Compound [2]Cl<sub>3</sub>.** [6]( $\text{PF}_6$ )<sub>2</sub> (30 mg, 0.023 mmol) and  $\text{AgPF}_6$  (15 mg, 0.060 mmol) were dissolved in a 3:5 acetone/ $\text{H}_2\text{O}$  mixture (8 mL). To this solution was added Hmte (156  $\mu\text{L}$ , 1.80 mmol). The mixture was refluxed under argon for 9 h in the dark, after which it was filtered hot over celite. Acetone was removed under reduced pressure upon which the crude product with  $\text{PF}_6^-$  counter ions precipitated in water. It was filtered, washed and dried.  $\text{PF}_6^-$  ions were exchanged by  $\text{Cl}^-$  by stirring a 1:1 acetone/water solution (20 mL) of the crude product [2]( $\text{PF}_6$ )<sub>3</sub> with ion-exchange resin DOWEX 22 (30 mg) for 4 h. After filtration of the resin, acetone was evaporated under reduced pressure, and water was removed using a freeze drier machine to afford [2]Cl<sub>3</sub> as a reddish purple powder (12 mg, 0.011 mmol, 43%).  $^1\text{H}$  NMR (300 MHz,  $\text{CD}_3\text{OD}$ , 298 K, *see Scheme 6.2 for proton attribution*)  $\delta$  (ppm) 9.80 (d, J = 6.1 Hz, 1H, 6A), 8.81 (d, J = 8.1 Hz, 1H, 3A), 8.57 (t, J = 8.7 Hz, 2H, 1R' + 3B), 8.39 (m, 2H, 10R' + 4A), 8.0-8.05 (m, 4H, 5R + 9R' + 7R' + 5A), 7.93 (t, 2H, 4B + 2R'), 7.86 – 7.73 (m, 5H, 3R + T33'' + T3' + T5'), 7.56 (m, 1H, 2R), 7.48 – 7.32 (m, 4H, 4R' + 4R + T4 + T4''), 7.27 (d, J = 7.2 Hz, 1H, 5B), 7.20 – 7.07 (m, 3H, 6B + T55''), 6.92 (d, J = 4.1 Hz, 2H, T6 + T6''), 4.46 (d, J = 5.5 Hz, 2H,  $\alpha$ ), 3.80 (t, 2H,  $\beta$ ), 3.69 (q, 8H,  $\delta$ ), 3.46(d, J = 5.7 Hz, 2H, HO- $\underline{\text{CH}_2}$ ), 3.25 (s, 3H,  $\gamma$ ), 1.81 (t, J = 5.8 Hz, 2H,  $\underline{\text{CH}_2}$ -S), 1.43 – 1.36 (s, 3H, S- $\underline{\text{CH}_3}$ ), 1.28 (t, J = 6.9 Hz, 12H,  $\epsilon$ ).  $^{13}\text{C}$  NMR (75 MHz,  $\text{CD}_3\text{OD}$ , 298 K)  $\delta$  (ppm) 173.90 (C=O), 168.19 (3R,8R), 159.51, 159.34, 159.30, 159.12, 158.99, 158.96, 157.22, 154.52 (6A), 153.41, 140.05, 139.95, 139.09, 137.18, 135.81, 135.50, 133.83, 133.34, 133.24, 131.33, 131.16, 129.59, 128.90, 127.22, 126.20, 125.81, 124.98, 115.35, 114.86, 112.95, 97.32, 60.46 ( $\alpha$ ), 47.05 ( $\beta$ ), 46.10 ( $\delta$ ), 46.08 (S- $\underline{\text{CH}_3}$ ), 39.53 ( $\gamma$ ), 38.51 (OH- $\underline{\text{CH}_2}$ ), 38.08( $\underline{\text{CH}_2}$ -S), 12.83 ( $\epsilon$ ). High resolution ES MS m/z (calc): 360.45788 (360.45780 [ $\text{M}-3\text{Cl}$ ] $^{3+}$ ), 540.18291 (540.18289 [ $\text{M}-3\text{Cl}-\text{H}$ ] $^{2+}$ ). UV-vis:  $\lambda_{\text{max}}$  ( $\epsilon$  in  $\text{L}\cdot\text{mol}^{-1}\cdot\text{cm}^{-1}$ ) in pure  $\text{H}_2\text{O}$ : 570 nm (44000).

### 6.5.3. Emission measurements

Three stock solutions of rhodamine B (solution **A**, 2.4 mg in 50 mL H<sub>2</sub>O, 1.0×10<sup>-4</sup> M), of compound [4]Cl (solution **B**, 3.8 mg in 50 mL H<sub>2</sub>O, 1.0×10<sup>-4</sup> M) and of compound [2]Cl<sub>3</sub> (solution **C**, 1.2 mg in 10 mL H<sub>2</sub>O, 1.0×10<sup>-4</sup> M) were prepared. 150 μL of stock solution **A**, 100 μL of solution **B**, or 120 μL of solution **C** was transferred into a quartz cuvette and was diluted to 3 mL by adding H<sub>2</sub>O using a micropipette (final concentrations: of **A'**: 5.0×10<sup>-6</sup> M, **B'**: 3.3×10<sup>-6</sup> M, **C'**: 4.0×10<sup>-6</sup> M). The absorbance of each solution was measured (A<sub>570</sub>=0.23 for all solutions). Emission spectra were recorded with the same excitation parameters (λ<sub>e</sub>=570 nm).

### 6.5.4. Irradiation experiments

**NMR measurements.** [2]Cl<sub>3</sub> (3.8 mg, 3.2 μmol) was weighed into an NMR tube and degassed D<sub>2</sub>O (0.60 mL) was added to the tube in the dark under argon. The <sup>1</sup>H NMR of the sample was measured as a reference, and irradiation at 452 nm or 570 nm was started at T=298 K using the beam of a LOT 1000 W Xenon arc lamp filtered with an Andover filter at the appropriate wavelength, and arriving on the side of the NMR tube. The temperature of the tube was kept constant by thermostat set at 298 K. After 220 minutes, 310 minutes, and 480 minutes of irradiation at 452 nm, or 170 minutes, 320 minutes, and 530 minutes at 570 nm, <sup>1</sup>H NMR spectra were measured. A reference sample was also prepared at the same concentration, and kept in the dark for comparison of their <sup>1</sup>H NMR spectra. Neither of these reference samples showed any observable conversion in the dark.

**UV-vis experiments.** 1 mL of a stock solution **D** of compound [2]Cl<sub>3</sub> (1.2 mg in 10 mL H<sub>2</sub>O, 1.0×10<sup>-4</sup> M) or 0.8 mL of a stock solution **E** of [1](BF<sub>4</sub>)<sub>2</sub> (1.7 mg in 5 mL H<sub>2</sub>O, 4.5×10<sup>-4</sup> M) was transferred into a UV-vis cuvette. The volume of the solution was completed to 3 mL with H<sub>2</sub>O (using a micropipette) in the dark (final concentration: **D'**: 3.4×10<sup>-5</sup> M, **E'**: 1.2×10<sup>-4</sup> M). The UV-vis spectrum of each sample was measured and afterwards the sample was irradiated at 452 nm or 570 nm using the beam of a LOT 1000 W Xenon arc lamp filtered by an Andover bandpass filter, and directed into a 2.5 mm diameter optical fiber bundle bringing the light vertically into the cuvette, *i.e.*, perpendicular to the horizontal optical axis of the spectrophotometer (*see Appendix I*). After each irradiation period (varying from 1 min to 3 min depending on the samples) a UV-vis spectrum was measured until a total irradiation time of 350 minutes and 82 minutes was reached, for **D'** and **E'**, respectively. The concentrations in [RuHmte] ([2]<sup>3+</sup> or [1]<sup>2+</sup>) and [RuOH<sub>2</sub>] ([7]<sup>3+</sup> or [8]<sup>2+</sup>) were determined by deconvolution knowing the extinction coefficients of both species (*see Appendix I*). The evolution of ln([RuHmte]/[Ru]<sub>tot</sub>) was plotted as a function of irradiation

time, and from the slope  $S$  of these plot  $k_{\phi}$  at  $\lambda_e=452$  nm or  $\lambda_e=570$  nm were determined to be  $1.9(3)\times 10^{-4}$  s $^{-1}$  and  $4.4(3)\times 10^{-4}$  s $^{-1}$ , for  $[2]^{3+}$ , respectively, and  $1.3(4)\times 10^{-4}$  and  $5.2(2)\times 10^{-5}$  s $^{-1}$  for  $[1]^{2+}$ , respectively. Knowing the photon flux and probability of photon absorption  $1-10^{-3A_e}$ , where  $3A_e$  is the absorbance of the solution at the excitation wavelength  $\lambda_e$ , the number of moles of photons  $Q$  absorbed at time  $t$  by RuHmte since  $t_{irr}=0$  was calculated. Plotting  $n_{RuHmte}$  (the number of moles of RuHmte complex  $[1]^{2+}$  or  $[2]^{3+}$ ) vs.  $Q$  gave a straight line in each case. The slope of this plot directly corresponds to the quantum yield of the photosubstitution reaction. The values for the photosubstitution quantum yields were  $9.2(3)\times 10^{-3}$  and  $8.5(3)\times 10^{-3}$ , respectively, for  $[2]^{3+}$  and  $1.6(4)\times 10^{-2}$  and  $1.1(4)\times 10^{-2}$ , respectively, for  $[1]^{2+}$ , at  $\lambda_e=452$  nm or  $\lambda_e=570$  nm, respectively (see Appendix I, Section AI.3.2).

## 6.6. References

- [1] C. R. Hecker, P. E. Fanwick, D. R. McMillin, *Inorg. Chem.* **1991**, *30*, 659-666.
- [2] V. Balzani, G. Bergamini, S. Campagna, F. Puntoriero, in *Photochemistry and Photophysics of Coordination Compounds I, Vol. 280* (Ed.: V. C. S. Balzani), **2007**, pp. 1-36.
- [3] B. A. McClure, E. R. Abrams, J. J. Rack, *J. Am. Chem. Soc.* **2010**, *132*, 5428-5436.
- [4] P. S. Wagenknecht, P. C. Ford, *Coord. Chem. Rev.* **2011**, *255*, 591-616.
- [5] E. Baranoff, J. P. Collin, J. Furusho, Y. Furusho, A. C. Laemmel, J. P. Sauvage, *Inorg. Chem.* **2002**, *41*, 1215-1222.
- [6] A. A. Rachford, J. J. Rack, *J. Am. Chem. Soc.* **2006**, *128*, 14318-14324.
- [7] S. Bonnet, J. P. Collin, J. P. Sauvage, E. Schofield, *Inorg. Chem.* **2004**, *43*, 8346-8354.
- [8] P. Mobian, J. M. Kern, J. P. Sauvage, *Angew. Chem. Int. Ed.* **2004**, *43*, 2392-2395.
- [9] J. Van Houten, R. J. Watts, *J. Am. Chem. Soc.* **1976**, *98*, 4853-4858.
- [10] P. C. Ford, *Coord. Chem. Rev.* **1982**, *44*, 61-82.
- [11] S. Bonnet, J.-P. Collin, *Chem. Soc. Rev.* **2008**, *37*, 1207-1217.
- [12] R. B. Sears, L. E. Joyce, M. Ojaimi, J. C. Gallucci, R. P. Thummel, C. Turro, *J. Inorg. Biochem.* **2013**, *121*, 77-87.
- [13] B. S. Howerton, D. K. Heidary, E. C. Glazer, *J. Am. Chem. Soc.* **2012**, *134*, 8324-8327.
- [14] R. N. Garner, J. C. Gallucci, K. R. Dunbar, C. Turro, *Inorg. Chem.* **2011**, *50*, 9213-9215.
- [15] S. Betanzos-Lara, L. Salassa, A. Habtemariam, O. Novakova, A. M. Pizarro, G. J. Clarkson, B. Liskova, V. Brabec, P. J. Sadler, *Organometallics* **2012**, *31*, 3466-3479.
- [16] A. J. Gomes, P. A. Barbougli, E. M. Espreafico, E. Tfouni, *J. Inorg. Biochem.* **2008**, *102*, 757-766.
- [17] F. Barragan, P. Lopez-Senin, L. Salassa, S. Betanzos-Lara, A. Habtemariam, V. Moreno, P. J. Sadler, V. Marchan, *J. Am. Chem. Soc.* **2011**, *133*, 14098-14108.
- [18] R. E. Goldbach, I. Rodriguez-Garcia, J. H. van Lenthe, M. A. Siegler, S. Bonnet, *Chem. Eur. J.* **2011**, *17*, 9924-9929.
- [19] N. J. Farrer, L. Salassa, P. J. Sadler, *Dalton Trans.* **2009**, 10690-10701.

- [20] H. M. Chen, J. A. Parkinson, S. Parsons, R. A. Coxall, R. O. Gould, P. J. Sadler, *J. Am. Chem. Soc.* **2002**, *124*, 3064-3082.
- [21] D. Crespy, K. Landfester, U. S. Schubert, A. Schiller, *Chem. Commun.* **2010**, *46*, 6651-6662.
- [22] A. Juarranz, P. Jaen, F. Sanz-Rodriguez, J. Cuevas, S. Gonzalez, *Clin. Transl. Oncol.* **2008**, *10*, 148-154.
- [23] A. P. Castano, P. Mroz, M. R. Hamblin, *Nat. Rev. Cancer* **2006**, *6*, 535-545.
- [24] A. M. Bugaj, *Photochem. Photobiol. Sci.* **2011**, *10*, 1097-1109.
- [25] P. Zhang, W. Steelant, M. Kumar, M. Scholfield, *J. Am. Chem. Soc.* **2007**, *129*, 4526-4527.
- [26] R. Weissleder, V. Ntziachristos, *Nat. Med.* **2003**, *9*, 123-128.
- [27] S. L. H. Higgins, K. J. Brewer, *Angew. Chem. Int. Ed.* **2012**, *51*, 11420-11422.
- [28] M. J. Rose, M. M. Olmstead, P. K. Mascharak, *J. Am. Chem. Soc.* **2007**, *129*, 5342-+.
- [29] M. J. Rose, N. L. Fry, R. Marlow, L. Hinck, P. K. Mascharak, *J. Am. Chem. Soc.* **2008**, *130*, 8834-8846.
- [30] N. L. Fry, J. Wei, P. K. Mascharak, *Inorg. Chem.* **2011**, *50*, 9045-9052.
- [31] N. L. Fry, P. K. Mascharak, *Acc. Chem. Res.* **2011**, *44*, 289-298.
- [32] J. P. Sauvage, J. P. Collin, J. C. Chambron, S. Guillerez, C. Coudret, V. Balzani, F. Barigelletti, L. Decola, L. Flamigni, *Chem. Rev.* **1994**, *94*, 993-1019.
- [33] K. Sienicki, W. L. Mattice, *J. Chem. Phys.* **1989**, *90*, 6187-6192.
- [34] P. Woolley, K. G. Steinhauser, B. Epe, *Biophys. Chem.* **1987**, *26*, 367-374.
- [35] M. H. Lim, S. J. Lippard, *Inorg. Chem.* **2004**, *43*, 6366-6370.
- [36] E. K. Kainmuller, E. P. Olle, W. Bannwarth, *Chem. Commun.* **2005**, 5459-5461.
- [37] M.-J. Li, K. M.-C. Wong, C. Yi, V.-W. Yam, *Chem. Eur. J.* **2012**, *18*, 8724-8730.
- [38] O. Filevich, B. Garcia-Acosta, R. Etchenique, *Photochem. Photobiol. Sci.* **2012**, *11*, 843-847.
- [39] H. N. Kim, M. H. Lee, H. J. Kim, J. S. Kim, J. Yoon, *Chem. Soc. Rev.* **2008**, *37*, 1465-1472.
- [40] M. Beija, C. A. M. Afonso, J. M. G. Martinho, *Chem. Soc. Rev.* **2009**, *38*, 2410-2433.
- [41] S. Burazerovic, J. Gradinaru, J. Pierron, T. R. Ward, *Angew. Chem. Int. Ed.* **2007**, *46*, 5510-5514.
- [42] J. del Marmol, O. Filevich, R. Etchenique, *Anal. Chem.* **2010**, *82*, 6259-6264.
- [43] R. A. Leising, S. A. Kubow, M. R. Churchill, L. A. Buttrey, J. W. Ziller, K. J. Takeuchi, *Inorg. Chem.* **1990**, *29*, 1306-1312.
- [44] C. A. Bessel, J. A. Margarucci, J. H. Acquaye, R. S. Rubino, J. Crandall, A. J. Jircitano, K. J. Takeuchi, *Inorg. Chem.* **1993**, *32*, 5779-5784.
- [45] A. Bahreman, B. Limburg, M. A. Siegler, E. Bouwman, S. Bonnet, *Inorg. Chem.* **2013**, *52*, 9456-9469.
- [46] M.-P. Santoni, A. K. Pal, G. S. Hanan, A. Proust, B. Hasenknopf, *Inorg. Chem. Commun.* **2011**, *14*, 399-402.
- [47] M. Kasha, *Discuss. Faraday Soc.* **1950**, 14-19.
- [48] A. Bahreman, B. Limburg, M. A. Siegler, R. Koning, A. J. Koster, S. Bonnet, *Chem. Eur. J.* **2012**, *18*, 10271-10280.
- [49] E. C. Constable, M. D. Ward, *Dalton Trans.* **1990**, 1405-1409.

